**NANOSIMS STUDIES OF DUST PROJECTILE SHOTS INTO STARDUST-TYPE AEROGEL AND ALUMINUM FOILS.** P. Hoppe[1], P. Heck[1], F. Hörz[2], J. Huth[1], K. K. Marhas[1,3], K. Messenger[2], C. Snead[4], and A. Westphal[4], [1]Max-Planck-Institute for Chemistry, Particle Chemistry Department, P.O. Box 3060, 55020 Mainz, Germany (hoppe@mpch-mainz.mpg.de), [2]NASA Johnson Space Center, Houston, Texas 77058, USA, [3]Laboratory for Space Sciences, Washington University, St. Louis, MO 63130, USA, [4]Space Sciences Laboratory, University of California at Berkeley, Berkeley, CA 94720, USA.

**Introduction:** Primitive meteorites and interplanetary dust particles (IDPs) contain nm- to μm-sized presolar dust grains that formed in the winds of evolved stars or in the ejecta of supernova explosions [1-3]. Except the presolar diamonds, whose circumstellar origin is still in question, presolar silicates make up the most abundant presolar grain type. Abundances of presolar silicates range up to >100 ppm in meteorites [4, 5] and sometimes even approach or exceed 1000 ppm in IDPs [6, 7]. Comets are believed to represent the most primitive matter in the Solar System and it is expected that the abundances of presolar grains in comets are at least as high as in IDPs. The Stardust space probe has collected cometary matter during the flyby of comet 81P/Wild 2 as well as contemporary interstellar dust [8, 9]. The laboratory study of this material provides a unique opportunity to get new insights into the nature of presolar grains and on the material from which our Solar System formed.

The Stardust space probe collected extraterrestrial matter with two different types of capture media, namely, low-density silica aerogel (1039 $cm^2$ surface area) and aluminum foil (Al 1100, 153 $cm^2$). Here, we report on a feasibility study of isotopic analyses on Stardust samples, aimed at the discovery of presolar grains, with the Cameca NanoSIMS 50 ion microprobe at MPI for Chemistry. Two types of samples were studied: (i) Crater residues on Stardust-type Al foils from impact experiments using particles from the Allende CV3 meteorite and soda lime glass. (ii) Ultramicrotome sections of Allende particles extracted from Stardust-type aerogel.

**Experimental:** Stardust-type Al foils and aerogel cells were bombarded with powdered Allende material (nominal size: 38-43 μm) with a velocity of ~6 km/s, using the 5 mm caliber Light Gas Gun at NASA JSC. Additional Al foils were bombarded with soda lime glass particles (nominal size: 8 μm). Selected Allende particles were extracted at SSL Berkeley from the aerogel using micro-tweezers. Ultra-microtome sections with thickness of ~100 nm of some of these particles were produced at JSC and SSL Berkeley and placed on TEM grids (Fig. 1). Seven and 3 craters (3-37 μm), respectively, produced by Allende and soda lime glass projectiles and 7 microtome sections (2 from sample B2, particle size 50x10 $μm^2$; 5 from sample E237-7f-s3g6, particle size ~25 μm) were selected for the NanoSIMS measurements. Prior to the NanoSIMS studies, all samples were documented in the SEM (Leo 1530 FESEM) (see Figs. 1-4).

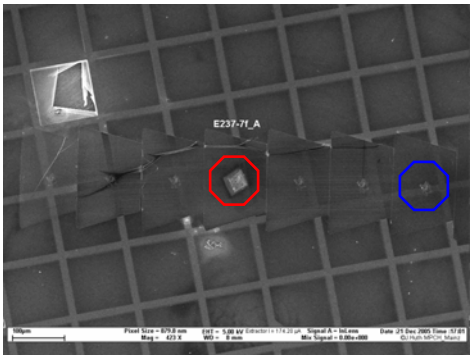


**Figure 1.** SEM image of ultra-microtome sections (E237-7f-s3g6) prepared from Allende projectiles extracted from aerogel. Red outline: NanoSIMS raster around section A. Blue outline: section D before NanoSIMS analysis.

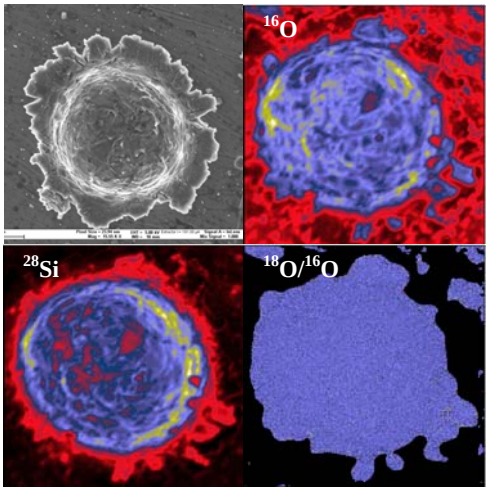


**Figure 2.** SEM image and NanoSIMS ion images of $^{16}O$, $^{28}Si$, and $^{18}O/^{16}O$ of a crater produced by a soda lime glass projectile. Field of view is 13 x 13 $μm^2$ in the ion images.

The NanoSIMS measurements were done with a $Cs^+$ primary ion beam (< 1 pA, ~100 nm) and parallel detection of $^{16}O$, $^{17}O$, $^{18}O$, $^{28}Si$, and $^{27}Al^{16}O$ (all samples) and of $^{12}C$, $^{13}C$, $^{12}C^{14}N$, $^{12}C^{15}N$, and $^{28}Si$ (4 Allende-bombarded Al foils). Surface contaminations

were removed by rastering a 20-25 pA $Cs^+$ beam for several minutes over the regions of interest prior to the isotope analyses. Ion images (256x256 to 512x512 pixels) with total integration times of up to several hours were acquired for whole particles/craters (Figs. 2-4) and for sub-areas (10x10 $\mu m^2$) of larger craters and the microtome sections (Fig. 5).

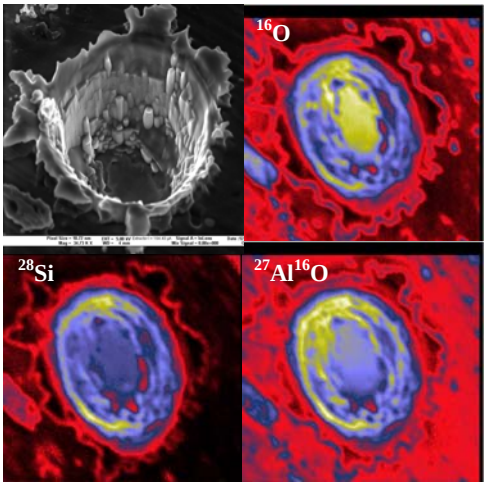


**Figure 3.** SEM image (after NanoSIMS analysis) and NanoSIMS ion images of $^{16}O$, $^{28}Si$, and $^{27}Al^{16}O$ of a crater produced by an Allende projectile. Field of view is 8 x 8 $\mu m^2$ in the ion images (from ref. 10).

**Results and discussion:** The NanoSIMS studies have shown that crater topograpy has only a little effect on lateral resolution, which is essentially given by the primary ion beam diameter (Figs. 2, 3). The same holds for the microtome sections studied here (Fig. 5). Instrumental mass fractionation varies only at the percent level across the craters or microtome sections (Figs. 2, 5) which does not pose a problem for the identification of presolar grains. For the O-isotopic ratios in the crater residues the counting statistical errors are ~10 % ($^{17}O/^{16}O$) and ~4 % ($^{18}O/^{16}O$) for 300-400 nm-sized sub-areas (the typical size of presolar grains). Carbon was found in isolated hotspots (150-500 nm) inside the craters. Counting statistical errors of $^{13}C/^{12}C$ ratios of these hotspots are several percent. For the O-isotopic ratios in the microtomed Allende particles, the counting statistical errors are ~12 % ($^{17}O/^{16}O$) and ~5 % ($^{18}O/^{16}O$) for 500 nm-sized sub-areas (the larger errors reflect lower average secondary ion intensities compared to the crater measurements).

In conclusion, the lateral resolution and precision of NanoSIMS O- and C-isotopic measurements achieved on Stardust-analogue samples are by far sufficient to identify presolar grains, which typically have $^{17}O/^{16}O$ and $^{13}C/^{12}C$ ratios of 2-3x (oxides, silicates) and 1.5-2x (SiC) solar, respectively [1-3]. The preparation and measurement procedures applied to both types of samples studied here can thus be considered suitable for the study of Stardust material.

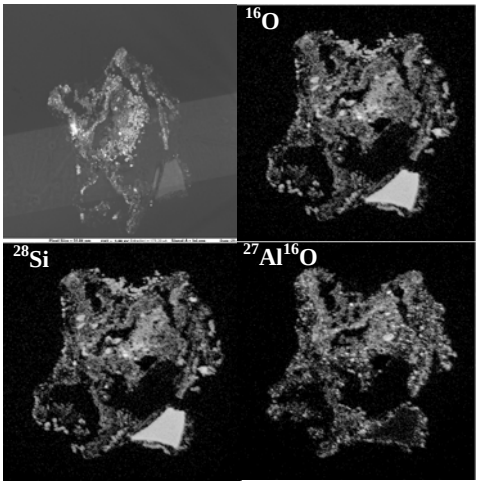


**Figure 4.** SEM image and NanoSIMS ion images of $^{16}O$, $^{28}Si$, and $^{27}Al^{16}O$ of ultra-microtome section E237-7f-s3g6-E. Field of view is 32 x 32 $\mu m^2$ in the ion images.

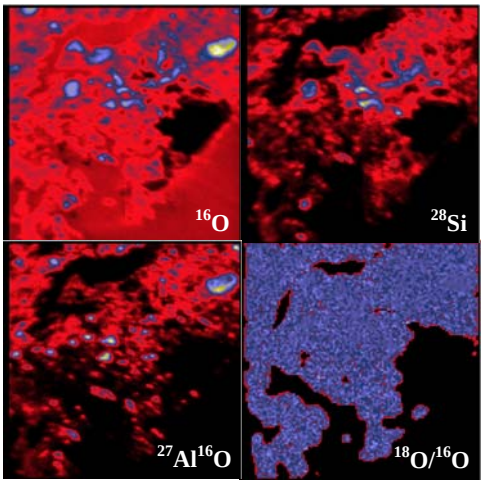


**Figure 5.** NanoSIMS ion images of $^{16}O$, $^{28}Si$, $^{27}Al^{16}O$, and $^{18}O/^{16}O$ of a 10 x 10 $\mu m^2$-sized sub-area of ultra-microtome section E237-7f-s3g6-E.

**References:** [1] Hoppe P. and Zinner E. (2000) *JGR*, 105, 10371. [2] Nittler L. R. (2003) *EPSL*, 209, 259. [3] Zinner E. (2004) in *Treatise in Geochemsitry* (eds. K. K. Turekian et al.), Elsevier, Oxford and San Diego, p. 17. [4] Nguyen A. N. and Zinner E. (2004) *Science*, 303, 1496. [5] Mostefaoui S. and Hoppe P. (2004) *ApJ*, 613, L149. [6] Messenger S. et al. (2003) *Science*, 300, 105. [7] Floss C. and Stadermann F. (2004) *LPS XXXV*, abstract #1281. [8] Brownlee D. E. et al. (2003) *JGR*, 108, E8111. [9] Tsou P. et al. (2003) *JGR*, 108, E8113. [10] Hoppe P. et al. (2006) *MAPS*, submitted.